Supporting Information

High-throughput Nuclear Delivery and Rapid Expression of DNA via Mechanical and Electrical Cell Membrane Disruption

Xiaoyun Ding[1,2,a], Martin Stewart[1,2,a], Armon Sharei[1,2], James C. Weaver[3], Robert S. Langer[1,2,*], and Klavs F. Jensen[1,*]

---

[1] Department of Chemical Engineering, Massachusetts Institute of Technology, Cambridge, MA 02139, USA

[2] The David Koch Institute for Integrative Cancer Research, Massachusetts Institute of Technology, Cambridge, MA 02139, USA

[3] Harvard–MIT Division of Health Sciences and Technology, Massachusetts Institute of Technology, Cambridge, MA 02139, USA

[a] These authors contributed equally to this work

[*] To whom correspondence should be addressed. Email: *rlanger@mit.edu*, *kfjensen@mit.edu*.

Device Fabrication

Two major steps were involved in the fabrication of the device (Fig. S1): (1) the fabrication of electrodes on the Pyrex wafer, and (2) the fabrication of microfluidic channel on the silicon wafer. Figure S1 (*a–d*) shows the fabrications of electrodes. A layer of photoresist (SPR3012, MicroChem, Newton, MA) was spin-coated on a 6 inch Pyrex wafer, patterned with a UV light source, and developed in a photoresist developer (MF CD-26, Microposit). A double-layer metal (Ti/Pt, 50Å/500Å) was subsequently deposited on the wafer using an e-beam evaporator (Semicore Corp), followed by a lift-off process to remove the photoresist and form the electrodes and pads. Two steps of photolithography were involved to fabricate silicon microfluidic channels, as shown in Fig. S1 (*e–h*). The silicon wafer was first patterned by photoresist (Shipley 1827, MicroChem, Newton, MA) and etched by a Deep Reactive Ion Etching (DRIE, Adixen, Hingham, MA). A second photolithography and DRIE were applied to etch through the silicon wafer to form the inlet and outlet for the microfluidic device.

Finally, silicon layer was sealed with Pyrex layer using anodic bonding at 300 °C and 800 V, and diced into separate chip with a dimension of 6×23 mm^2. The bottom panel of Figure S1 shows the final device. The width of electrode finger and spacing gap of device used in our setup are 40 μm and 60 μm, respectively. The height of the microfluidic channel in the silicon substrate is 20 μm.

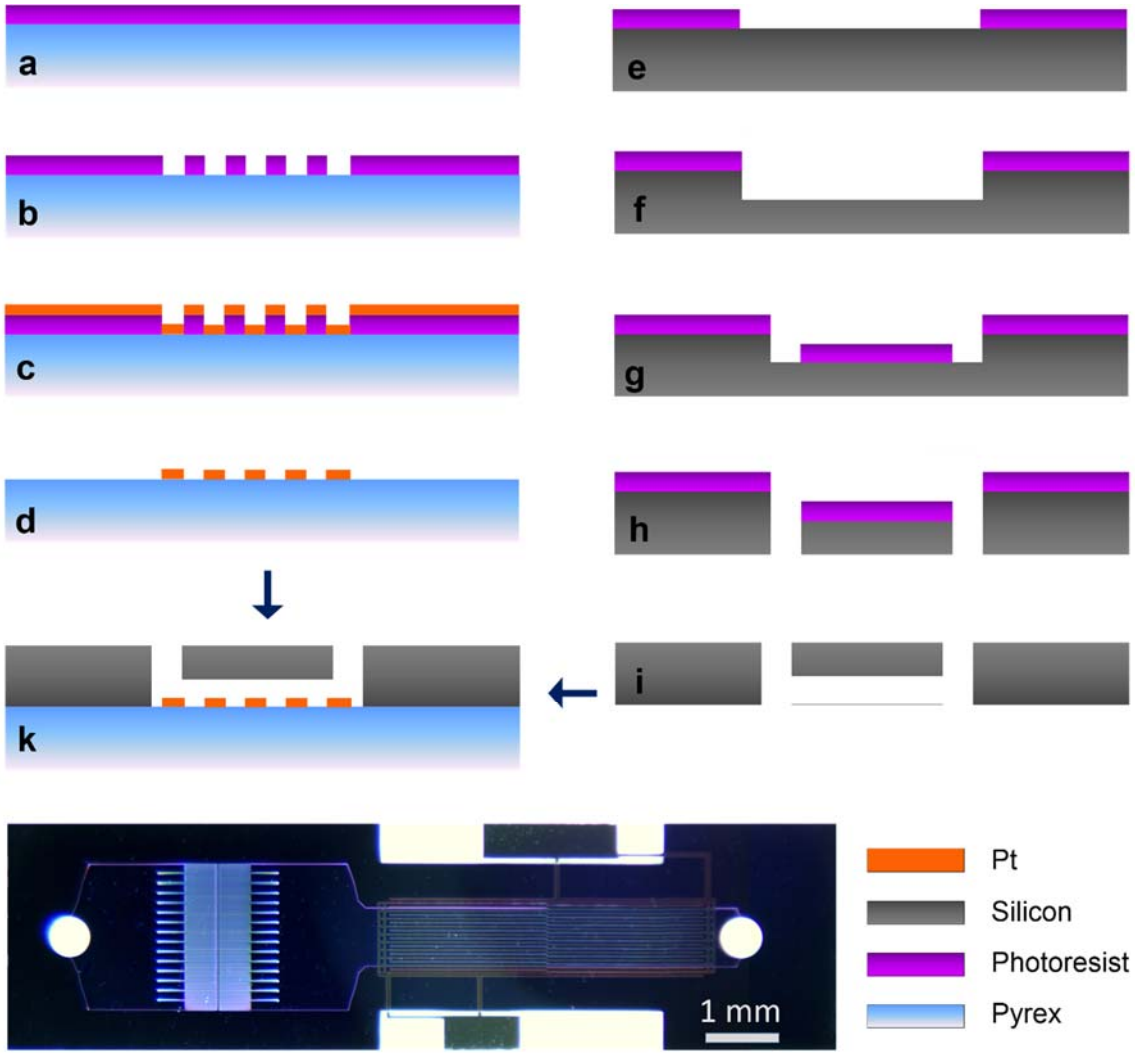

Figure S1 Device fabrication process. (*a*–*d*) Fabrication of the electrodes on a Pyrex layer includes a metal deposition process and a following lift-off process. (*e*–*i*) Fabrication of microchannels on silicon wafer using lithography and DRIE processes twice. (k) The bonding between the silicon substrate and the Pyrex layer. The bottom figure shows the final device.

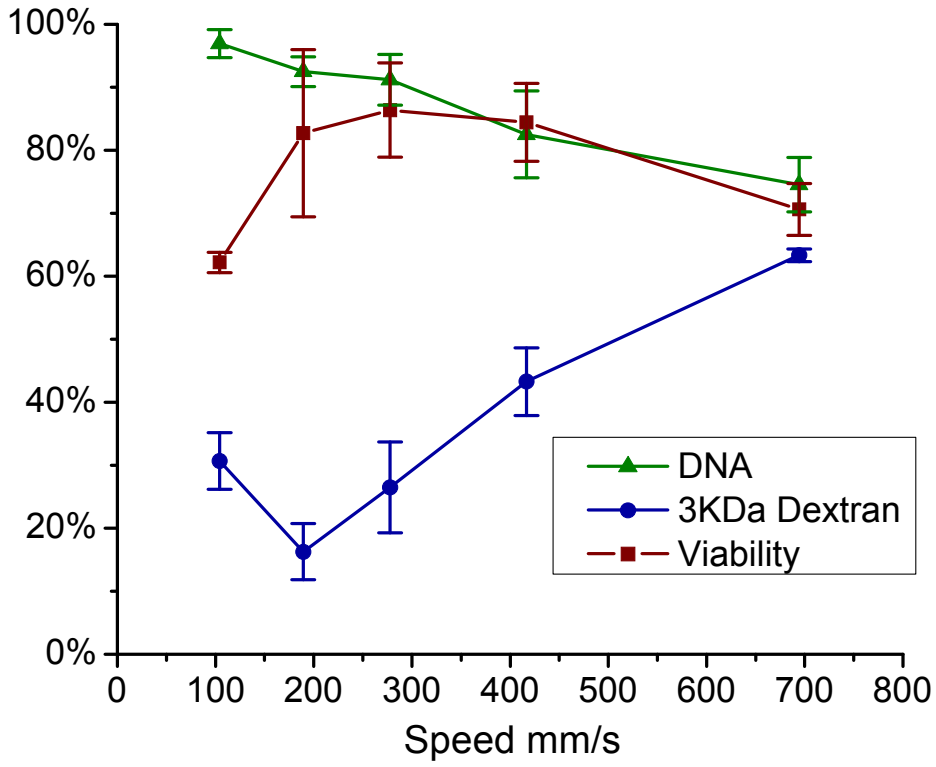

Figure S2 Delivery performance depends on cell speed. Delivery efficiency of 3K Da dextran, DNA transfection efficiency, and cell viability were measured 24 hours after treatment. A 10-7 DFE chip was used and the electric pulse of 0.1ms (200Hz) at 10 V. The yield of DNA transfection is maximum near the cell speed of 300 mm/s. Each data point was the mean value of triplicate and error bars represent ± s.d.

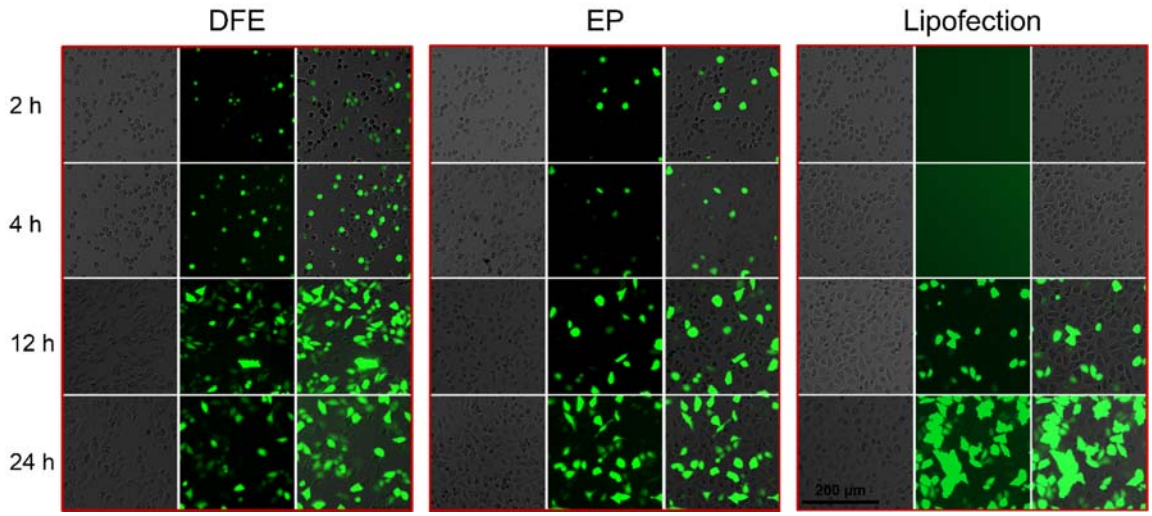

Figure S3 Fluorescence images of Hela cells. Comparison of the expression of GFP plasmid DNA by DFE, EP, and Lipofection. Fluorescence microscopy images of cells shows that GFP expression occurred much faster in DFE than in EP and Lipofection.

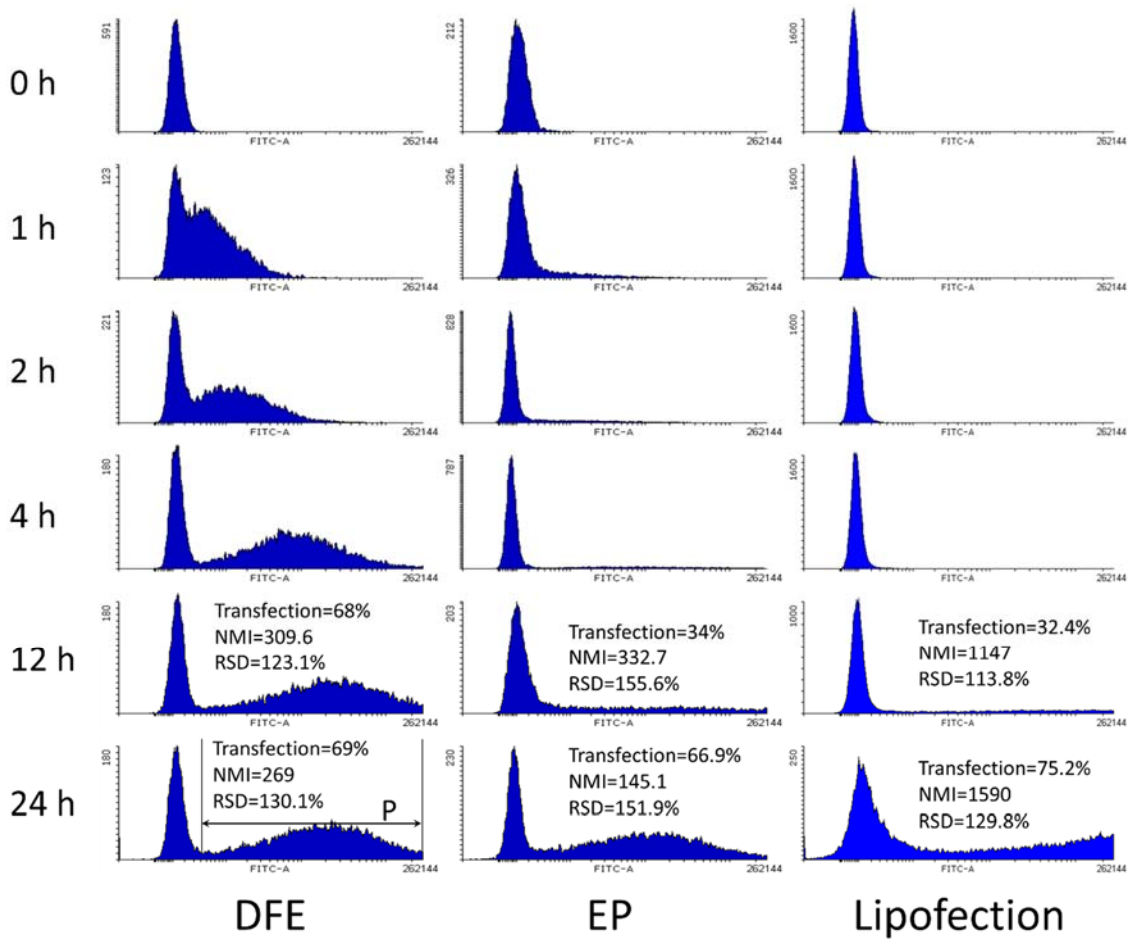

Figure S4 Histogram of GFP fluorescence intensity after DNA transfection. The GFP fluorescence intensity distribution of Hela cells measured by flow cytometry at different time points post treatment. The results indicate that in DFE, DNA transcription occurs rapidly after delivery. In EP and Lipofection, intracellular transport of DNA requires hours before the DNA is accessible to transcription. Statistical analysis NMI (normalized mean intensity) and RSD (relative standard deviation) were carried out based on the sample within gating P, indicating DFE has a better balance between transfection level and uniformity.

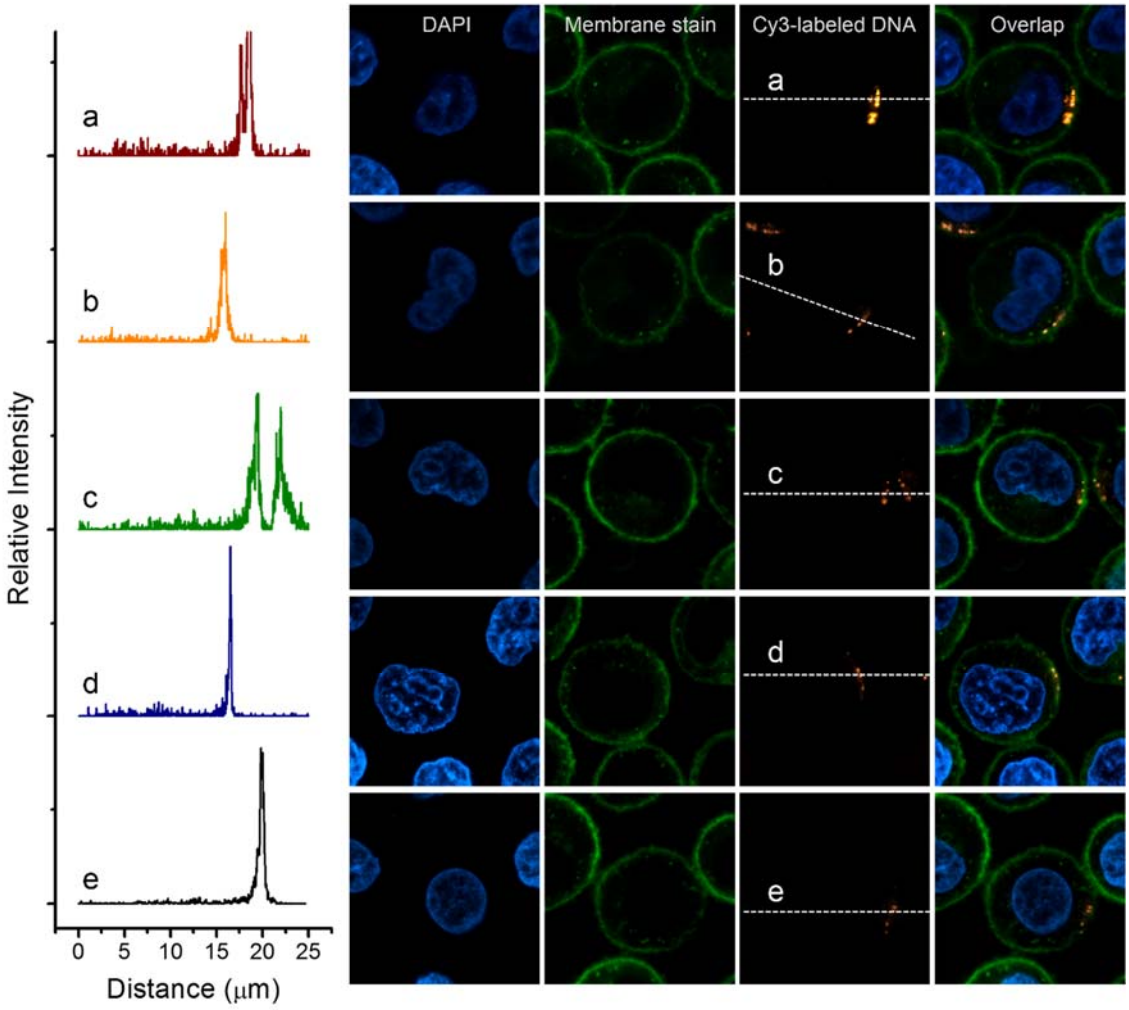

Figure S5 5 Repeats of direct visualization of CY3 fluorescence labeled DNA plasmid transfer into Hela cells by confocal fluorescence microscopy after EP (electroporation). Hela cells were mixed with DNA and treated by NEON electroporation. After treatment, cells were incubated in culture medium for 3 minutes, washed, fixed, and imaged by confocal microscopy. The results show that strong signal of DNA molecule aggregations were detected only at the plasma membrane while no detectable DNA was found within cells. Left panel shows the fluorescence profile along the dashed line across each single cell on the raw data images of a-e. The contrast of images have been adjusted for better readability.

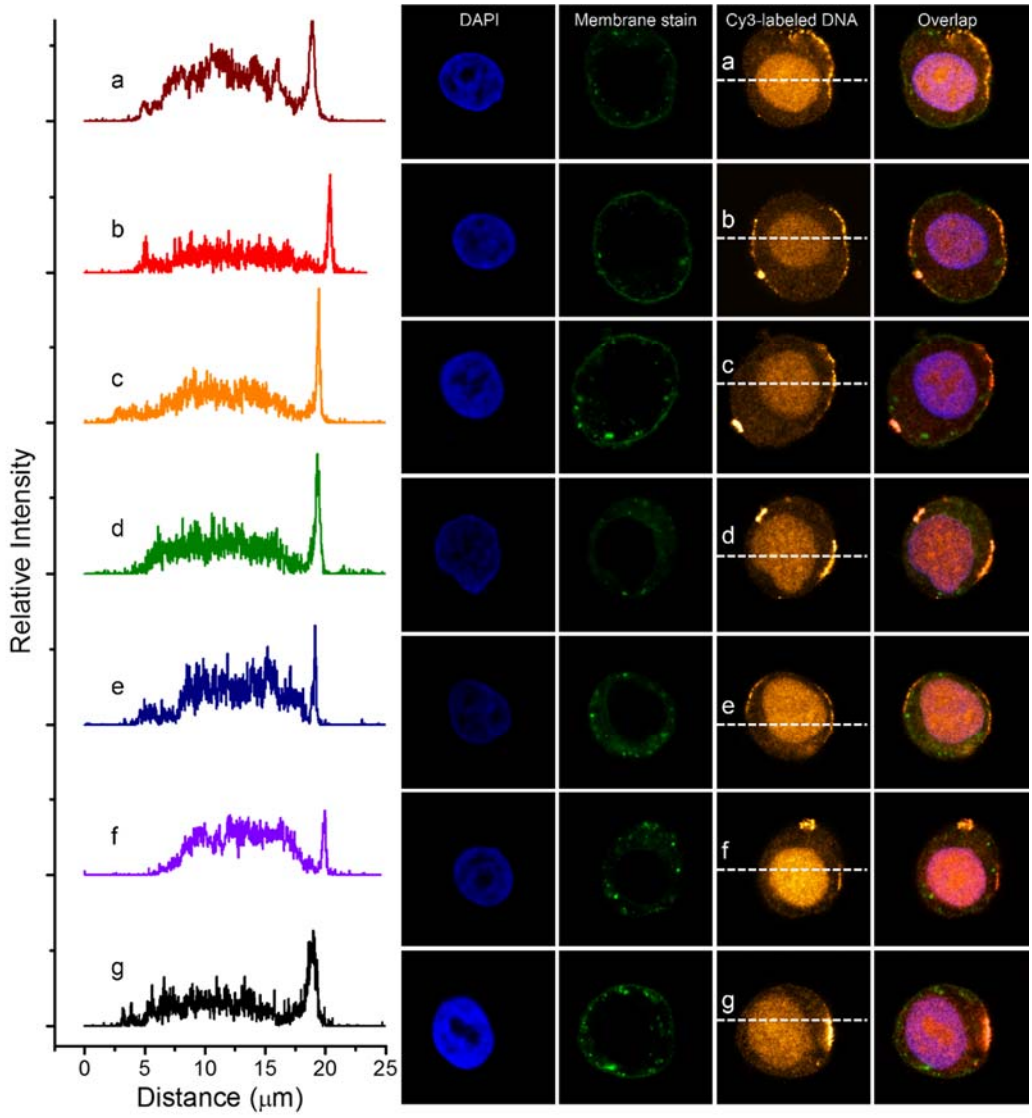

Figure S6 7 Repeats of direct visualization of CY3 fluorescence labeled DNA plasmid transfer into Hela cells by confocal fluorescence microscopy after DFE. Hela cells were mixed with DNA and treated by DFE. After treatment, cells were incubated in culture medium for 3 minutes, washed, fixed and imaged by confocal microscopy. The results show that DNA was distributed over cell nucleus and cytoplasm. DNA molecules aggregates were also observed at the plasm membrane as in electroporation. Left panel shows the fluorescence profile along the dashed line across each single cell on the raw data images of a-g. The fluorescence intensity in nucleus is stronger than that in cytoplasm. The contrast of fluorescent images have been adjusted for better readability.

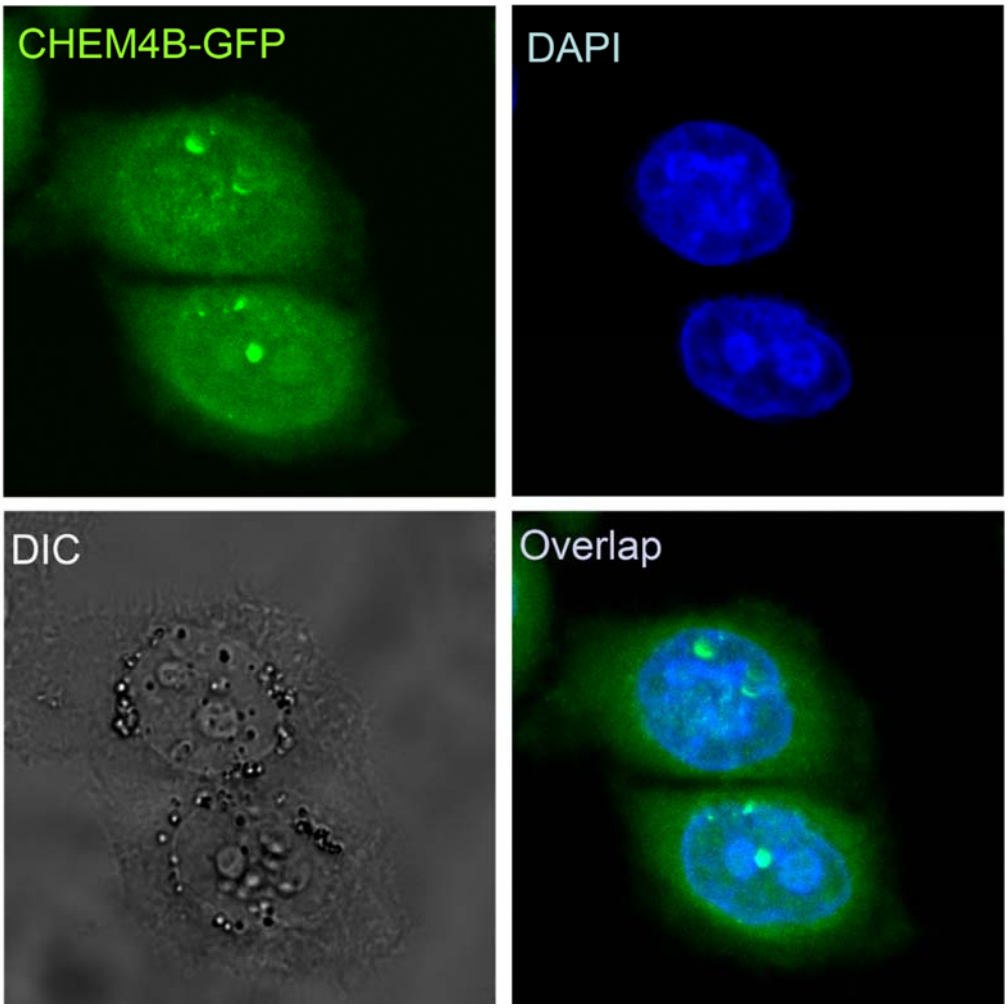

Figure S7 ESCRT-III are recruited to sites of microinjection wounding at nuclear envelope. Confocal images of HeLa cells expressing CHMP4B-GFP. Each cell was poked by microinjection needle for 2-3 times to generate wounds at nuclear envelope. Cells were fixed 3 minutes after microinjection. Cell nucleus were stained with DAPI.

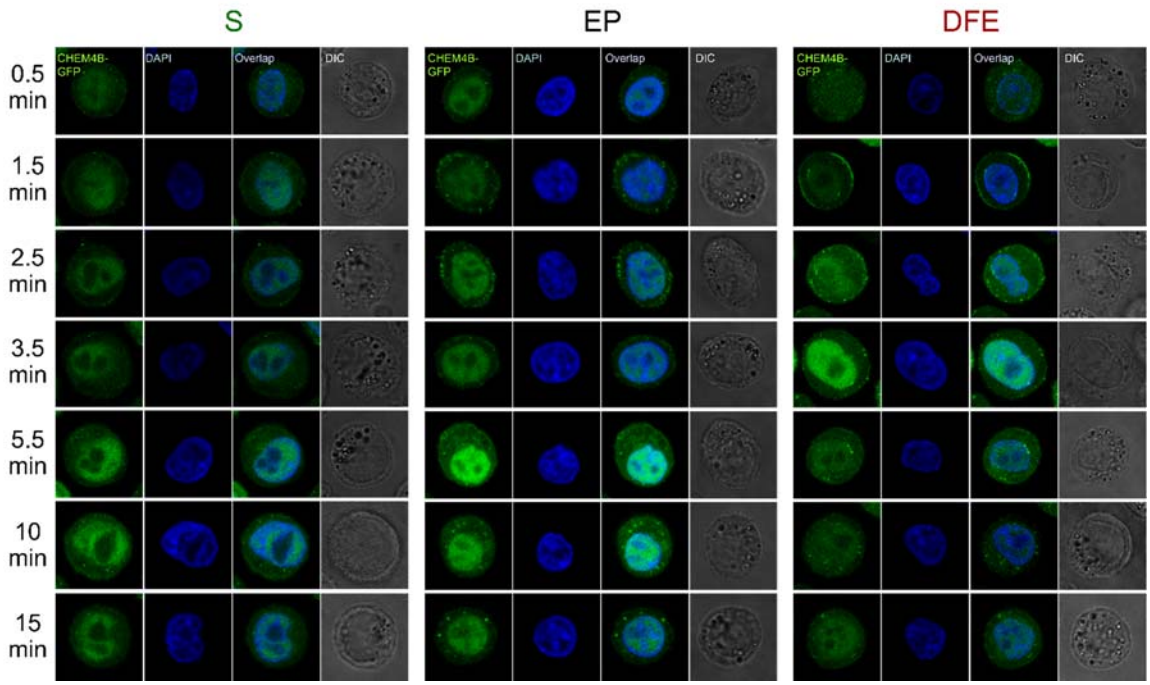

Figure S8 ESCRT-III recruitment at both plasma membrane and nuclear envelope following membrane disruption. Images of representative HeLa cells expressing GFP tagged CHMP4B, an important subunit of ESCRT-III complex. Cells were incubated in culture medium immediately after treatment of S (squeezing), EP (electroporation), or DFE, and fixed after incubation for 0.5, 1.5, 2.5, 3.5, 5.5, 10, and 15 minutes, for imaging using confocal microscopy. The results clearly indicate that membrane disruption and repair were found at both nuclear and plasma membrane after DFE. In S and EP, however, only plasma membrane disruption and repair were found.

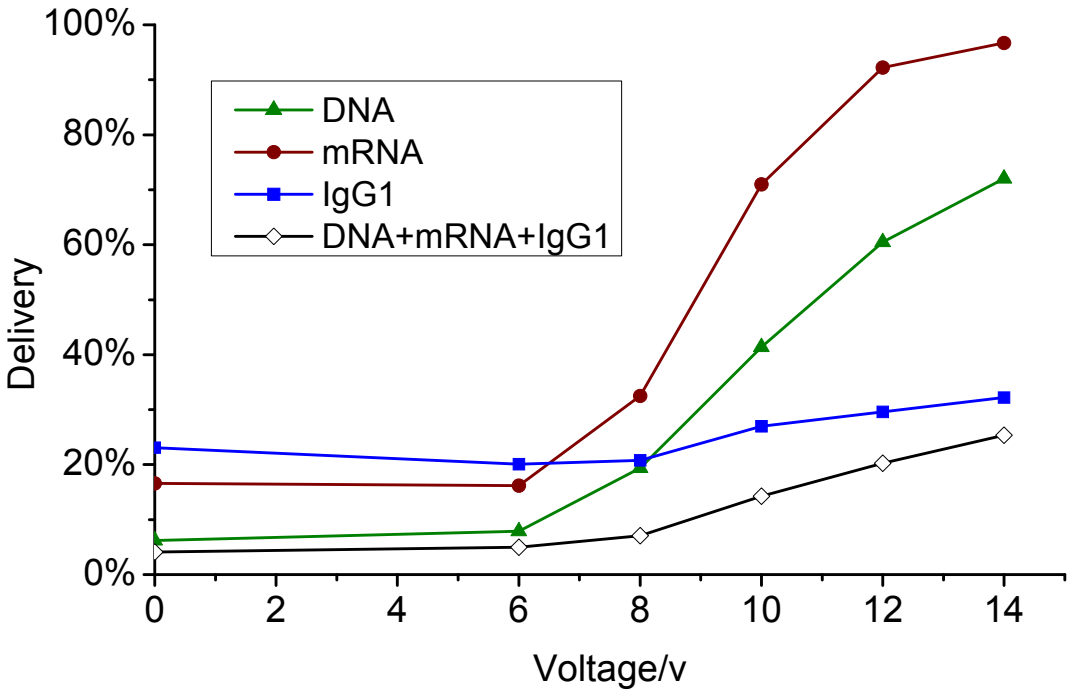

Figure S9 Co-delivery of DNA, mRNA, and protein (APC mouse IgG1 k Isotype Ctrl antibody). Hela cells were mixed with GFP plasmid DNA, RFP mRNA, fluorescent labeled protein and treated with DFE at different pulse strength. After treatment, cells were incubated for 24 hours and analyzed using flow cytometry. The results show that increasing voltage significantly promotes the transfection of DNA and mRNA. The protein delivery, however, increased slightly even at the maximum voltage, indicating that protein delivery is much more dependent on the mechanical disruption than the electrical delivery.

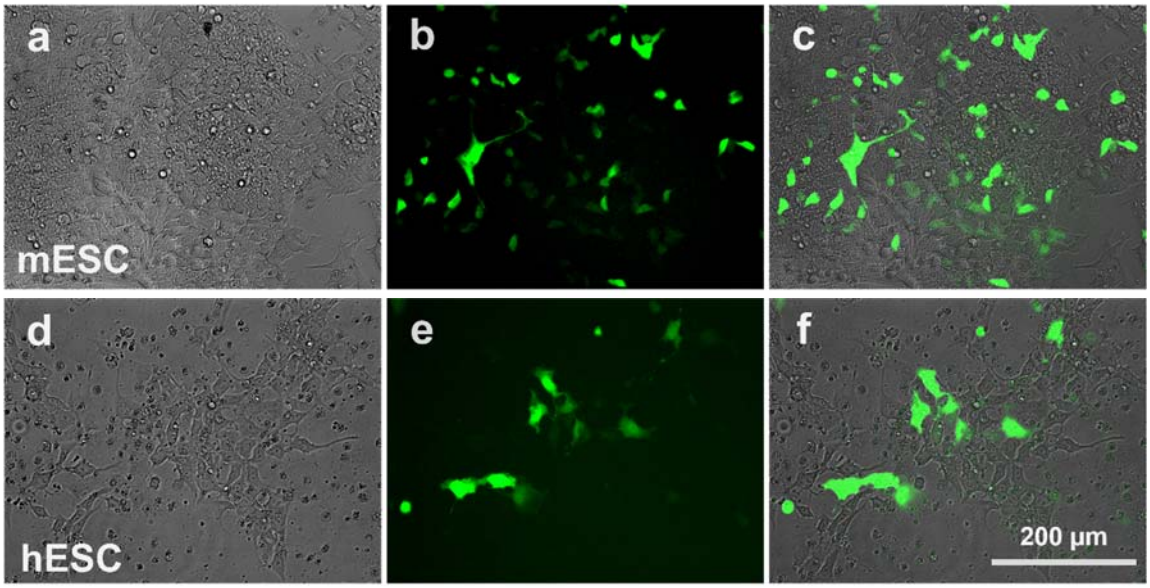

Figure S10 Fluorescence images of mESC and hESC. Expression of GFP plasmid DNA in mouse Embryonic Stem Cells (mESC) and human Embryonic Stem Cells (mESC) by DFE. **a**, **b**, and **c** show the bright field, fluorescence, and overlapped microscopy images of mESC treated by DFE with 19% of DNA transfection and 96% of viability. **d**, **e**, and **f** show the bright field, fluorescence, and overlapped microscopy images of hESC (human Embryonic Stem Cells) treated by DFE with 35% of DNA transfection and 60% of viability.